Effects of Azimuthal Control Jets on the structures of a Jet in Crossflow by Means of Proper Orthogonal Decomposition

Apichet Srimekharat* and Asi Bunyajitradulya

Department of Mechanical Engineering, Faculty of Engineering, Chulalongkorn University, Bangkok 10330, Thailand
*Corresponding Author: E-mail: t_apichet@hotmail.com, Tel: 02 218 6645, Fax: 02 218 6645

Abstract

The effects of azimuthal control jets on the structures of a jet in crossflow are investigated by Proper Orthogonal Decomposition (POD) analysis. The baseline jet in crossflow (JICF) has the effective velocity ratio (r) of 3.9, the crossflow Reynolds number (Re_{cf}) of 5,900, and the initial jet velocity profile fully developed turbulent. In the case of a controlled jet in crossflow (I15), azimuthal control jets are steadily deployed at the azimuthal positions $\theta = \pm\ 15^{\circ}$ and the control jets to main jet mass flowrate ratio r_m is 2%. Stereoscopic particle image velocimetry (SPIV) is used to acquire the three components of velocity vector in the cross planes. In order to isolate and identify the jet structures, which are defined here as the structures that are at least partly composed of the main jet fluid, only the main jet - and not the crossflow – is seeded with tracer particles. The results show that when the azimuthal control jets are applied, the most dominant modes change significantly. This effect is accompanied by the redistribution of energy among modes: from broad and low-profile in JICF to narrow and high-profile in I15, i.e., the energy becomes more concentrated in the first few modes. This indicates that the control jets have an effect in promoting and energizing a few dominant modes, in this case mode 1, over other modes when compared to JICF.

***Keywords**:* jet in crossflow, azimuthal control jets, proper orthogonal decomposition (pod), dominant structures, redistribution of energy

1. Introduction

Jet in crossflow (JICF) is the jet that is injected normally into a crossflow. It has wide range of applications, for example, in injectors for entrainment, mixing, and combustion of fuel and air, in gas turbine blades for film cooling. In these applications, the performance of the equipments depends on the jet characteristics such as trajectory, entrainment, and mixing. These characteristics in turn are the results of the interactions of the jet with the crossflow and the resulting jet structures. In this regard, the knowledge of the dominant jet structures can shed some lights on the efficient design and development of these equipments. On the other hand, various flow control techniques have been investigated in order to manipulate and control these jet structures so that certain desired outcomes such as the control of the jet trajectory and the enhancement of entrainment and mixing are achieved.

In regard to the jet structures and the jet characteristics, Smith and Mungal [1] found that, although the counter-rotating vortex pair (CVP) is the main mechanism for entrainment in the far field, it is the formation of the CVP in the near field that results in enhancement of entrainment and mixing of a JICF over a free jet. Yuan *et al*. [2], and Bunyajitradulya and Sathapornnanon [3] found that the formation of the CVP or the large-scale structure in the flow is closely related to the formation of flow shear layers near the jet exit. In addition, Yuan *et al*. [2] also described the origin of the CVP as developing from hanging vortices, which are formed in the skewed mixing layer at each lateral edge of the jet. Yuan and Street [4] described a close relation between the jet trajectory and its entrainment. In this regard, it is mentioned that in order to investigate the mixing structures of JICF more directly, Chongsiripinyo *et al*. [5], Limdumrongtum *et al*. [6], Watakusin *et al*. [7] have used condensation product formation technique to study JICF mixing structures in the top-view planes (plane perpendicular to the main jet axis) while Yingjaroen *et al*. [8] have used acid-base reactive product formation technique together with the passive scalar technique to study spanwisely-integrated mixing structures of JICF. The interest reader is referred to the references for further details.

In regard to attempts to manipulate and control various characteristics of JICF, many flow control techniques have been studied. Examples are using tab: Zaman and Foss [9], and Bunyajitradulya and Sathapornnanon [3]; using swirl: Niederhaus *et al.* [10], Wangjiraniran and Bunyajitradulya [11], Bunyajitradulya and Sathapornnanon [3], Denev *et al.* [12]; using pulsing: Hermanson *et al*. [13], Eroglu and Breidenthal [14], and M'Closkey *et al*. [15]; and using azimuthal control jets: Kornsri *et al*. [16]. Briefly, for local excitation at the jet exit such as the placement of tabs or azimuthal control jets, it is found that the excitation on the windward side causes the jet trajectory to be lowered; while on the leeward side, higher (Zaman and Foss [9], Bunyajitradulya and Sathapornnanon [3], and Kornsri *et al*. [16]). For swirl, it is found that, while swirl significantly affects JICF structures, causing it to be asymmetric, it has little effect on decay, suggesting that it has little effects on overall entrainment and mixing (e.g., Niederhaus *et al.* [10], and Wangjiraniran and Bunyajitradulya [11]). For pulsing, it is found that pulsing can significantly affect jet penetration and structures (M'Closkey *et al*. [15]). For azimuthal control jets, besides affecting the jet trajectory as mentioned, Kornsri *et al*. [16] also found that the deployment of the control jets at the defined optimal condition, $\theta = \pm 15^o$, which gives the lowest trajectory also has the effect in suppressing (the development of) the windward jet shear layer while promoting (the development of) the lateral skewed mixing layers, later developing into two dominant counter-rotating streamwise vortical structures (or the counter-rotating vortex pairs) – one on each lateral side. For further details, the reader is referred to the respective reference.

In order to extract the most dominant structures in JICF, Meyer *et al.* [17] used proper orthogonal decomposition (POD) on velocity field. They found that for JICF with r = 3.3 the wake

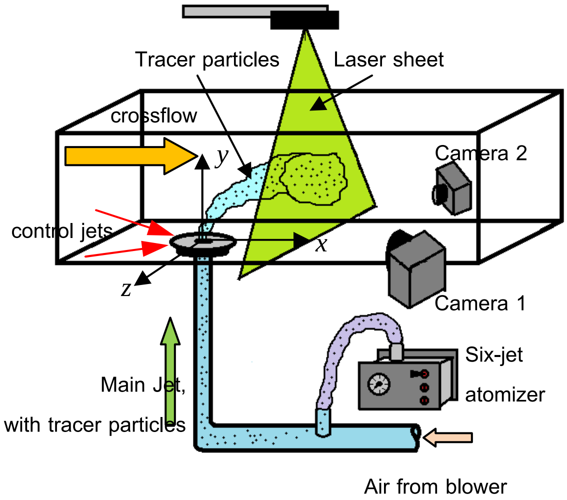

Fig. 1. Experimental setup and SPIV configuration.

vortices are the dominant structure while for JICF with r = 1.3 the jet shear-layer vortices are the dominant one.

With an attempt to manipulate and control trajectory and entrainment of JICF, we choose to study JICF and JICF controlled by azimuthal control jets, following Kornsri et al. [16]. The reasons for choosing azimuthal control jets as the flow control technique are that it has the potential to be used as an active flow control, it consumes relatively less energy, it can potentially withstand harsh environment, and its relative ease of implementation in engineering equipments.

As the performance of engineering equipments depends on the jet characteristics such as trajectory, entrainment, and mixing, which in turn depend on the jet structures, this work has an objective in investigating the effect of azimuthal control jets on JICF structures. In order to achieve this, we experiment with both the baseline JICF and the optimally controlled JICF (I15) in the sense of the controlled JICF with the lowest jet trajectory as described by Kornsri *et al*. [16]. In this controlled JICF case (I15), the azimuthal control jets are deployed steadily at the azimuthal position $\theta = \pm 15^{\circ}$ and the total control jets to main jet mass flowrate ratio r_m of 2%. The velocity fields at cross planes are then measured with stereoscopic particle image velocimetry (SPIV). We then analyze the jet structures using POD performed on the three-component velocity field data obtained from SPIV.

Of particular note in this work is the following. In order to isolate and identify the jet structure, which is here defined as the region in which its volume is at least partially composed of the main jet fluid, in measuring the velocity field with SPIV only the main jet fluid – and not the crossflow - is seeded with tracer particles. In this regard, the SPIV registers only the velocity in the jet and none in the region in which there is purely crossflow fluid. This work then differs from Meyer *et al.* [17], in which both the jet and the crossflow fluids are seeded, in this respect.

2. Experimental Setup

The experimental setup is similar to Kornsri et al. [16], with some modification to accommodate for the use of SPIV (Fig. 1). Briefly, the crossflow is generated in a blower tunnel with 50×50 cm^2 test section, which is 240 cm in length. The main jet and the azimuthal control jets header assembly is the same as that of Kornsri *et al*. [16] (Fig. 2). The diameters of the main jet (d) and the azimuthal control jets (d_{cj}) are 22.5 and 1 mm, respectively. The main jet pipe is modified from Kornsri *et al.* [16] such that it is a straight pipe of 44 d in length leading to

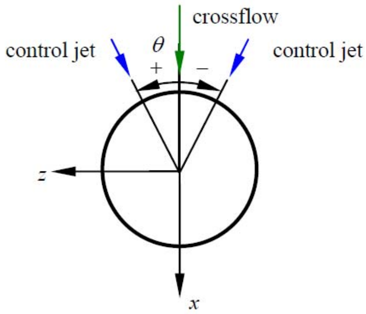

(a) Top view.

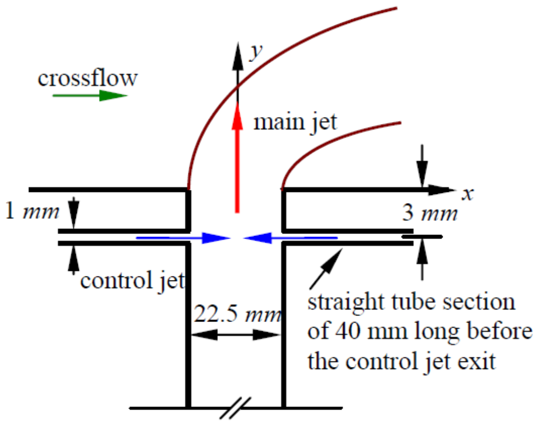

(b) Side view.

Fig. 2. The main jet and the control jets configuration.

the jet exit; this ensures the fully-developed turbulent pipe flow profile for the initial velocity profile of the main jet at the jet exit. Far away upstream in the supply air pipe leading to the main jet pipe, tracer particles for SPIV are seeded. The tracer particles are 5% glycerol solution, seeded with TSI™ six-jet atomizer (model 9306A), for which only one of the six jets is used.

All three components (V_x, V_y, V_z) of the velocity field in the cross planes (yz -plane) are measured with TSI™ SPIV system. The coordinate system used in this experiment is shown in Fig. 1, where x is the streamwise coordinate (in the crossflow direction), y is the transverse coordinate, and z is the spanwise coordinate; the origin of the coordinate system is at the center of the jet at the jet exit plane. For SPIV, the laser is New Wave Research Nd:YAG laser (model Solo 200XT), which generates nominal energy of 200 mJ at 532 nm. Light arm (model 610015) and light sheet optics (model 610021-SIL, -25 mm cylindrical and +500 mm spherical) are used to deliver the laser pulse from the laser head to the test section as laser sheet. Two identical CCD cameras (PowerView Plus11MP, model 630062) are used for imaging the flow field. The CCD has pixel resolution 4008 $\times$ 2672 pixels, pixel size 9 μm $\times$ 9 μm, image size 36.07 $\times$ 24.05 mm^2, and intensity dynamic range 12 bits. For each camera, the imaging lens is Tokina Macro 100 mm f2.8D for all measurement planes. Laser, cameras, and computer are synchronized with a synchronizer (model 610035). The acquisition is made through TSI™ Insight 4G software, with the acquisition rate of 2.07 Hz and the total of 4,000 velocity fields (2 $\times$ 4,000 particle images for each camera). In processing for velocity data from pairs of particle images, the initial interrogation area of 64 pixel $\times$ 64 pixel is used with overlap of 50%, resulting in the final interrogation area of 32 pixel $\times$ 32 pixel. For all cross planes measured (x/rd = 0.5 to 1.5), these parameters result in the velocity vector more than 10,000 vectors per field and the spatial resolution of the velocity vectors ranges from 1.09 mm $\times$ 1.09 mm at x/rd = 0.5 to 1.27 mm $\times$ 1.27 mm at x/rd = 1.5.

The experiment is conducted at the main jet average velocity V_j of 16.9 $\pm$ 0.8 m/s, the crossflow velocity V_{cf} of 4.3 $\pm$ 0.2 m/s, and the jet initial velocity profile fully-developed turbulent. These result in the effective velocity ratio r of 3.9 $\pm$ 0.3 and crossflow Reynolds number Re_{cf} of 5,900. For the controlled JICF case (I15), the azimuthal control jets are steadily deployed at the azimuthal position $\theta = \pm 15°$ and the total control jets to main jet mass flowrate ratio r_m of 2%.

Finally, the acquired 4,000 three-component planar velocity fields (snapshots) are analyzed with POD. The scheme used is as described in Meyer *et al.* [17].

3. Results and Discussion

Before we discuss the results, it is first emphasized that in this work we attempt to isolate and identify the jet extent and structures. We then define the jet extent as the region in which its volume is at least partly composed of the main jet fluid; therefore excluding the region in which its volume contains purely crossflow fluid, which is referred to as the crossflow region. Note that there can be some velocity fluctuation and disturbance in the crossflow region due to the interaction between the jet and the crossflow at their interface; nonetheless, this is excluded. Hence, only the main jet fluid is seeded while the crossflow fluid is not seeded with tracer particles. As a result, the SPIV registers only the velocity vectors in the jet, and none in the crossflow. Consequently, the POD results of SPIV data reflect only the jet structures in such region. Finally, note that in this preliminary analysis, the POD is performed on the fluctuating velocity component, for which the time mean (and not the conditional mean) is subtracted. Therefore, the resulting energy from the analysis reflects such kinetic energy of velocity fluctuation.

Figure 3 shows the POD modes for JICF and I15 at the planes x/rd = (a) 0.5 and (b) 1. The in-plane velocity components are presented as velocity vectors while the out-of-plane velocity component as contours. The percentage below each mode is the percentage of mode energy to total kinetic energy of velocity fluctuation, which is ordered consecutively from the highest energy in mode 1 to lower energy in the higher mode. In order to emphasize the out-of-plane velocity structures the contour colors are specific to case (JICF or I15) and plane but common among different modes of the same case and plane.

POD Modes

Figure 3 shows POD modes 1 and 2 at planes x/rd = 0.5 and 1, together with the contours of normalized mean speed $V/V_{cf} = \sqrt{V_x^2 + V_y^2 + V_z^2}/V_{cf}$ on the first row. For JICF at plane x/rd = 0.5, mode 1 has a shape of side lobes with additional two inner side lobes, especially the V_x component, while mode 2 has only side lobes. When the jet develops to x/rd = 1, the shape of mode 1 and mode 2 are interchanged.

When the control jets are applied (I15), however, at plane x/rd = 0.5 mode 1 changes significantly in shape; it penetrates less into the crossflow while expands more in the spanwise direction. This is similar to the results on the mean velocity by Kornsri *et al*. For mode 2, finer structures appear, the characteristic that is also observed in the modes of JICF. Overall, we

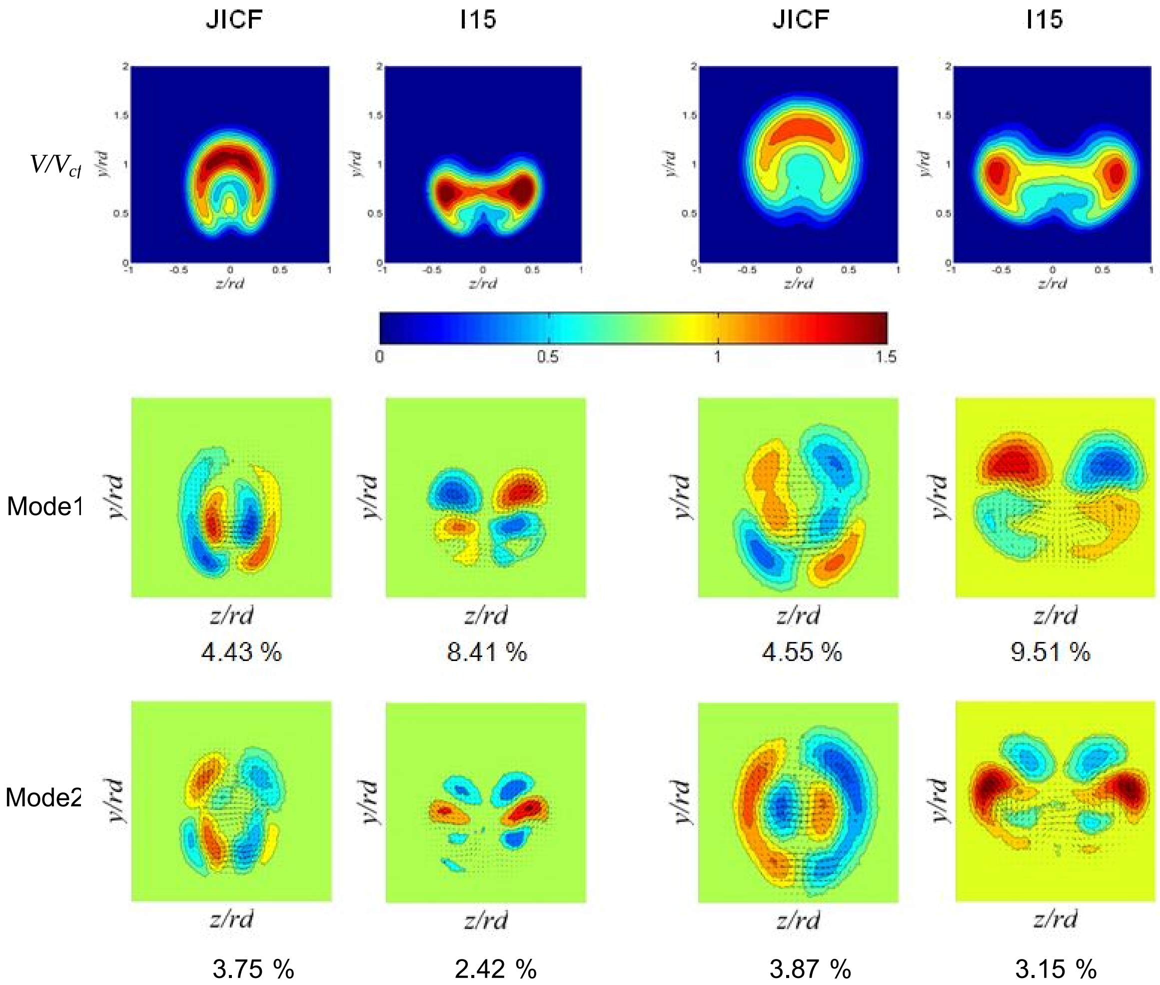

(a) x/rd = 0.5. (b) x/rd = 1.

Fig. 3. POD modes 1 and 2 for JICF and I15 at planes x/rd = (a) 0.5, (b) 1. The percentage below each mode indicates the percentage of mode energy to total energy. Contours of normalized mean speed (V/V_{cf}) are also shown in the first row.

observe that as the mode increases, the structure becomes finer in details.

Of particular interest is, however, the relative energy among modes. Specifically, for JICF the percentages of energy of mode 1 and 2 are comparable in all planes. However, when the control jets are applied, the percentage energy of mode 1 becomes much larger - by approximately three times - of mode 2 in all planes observed. This effect of the control jets in redistributing the energy among modes is discussed next.

Energy Distribution among Modes and Accumulative Energy

Figure 4 shows the distribution of energy among modes in terms of the percentage of mode energy to total energy (e) in relation to mode number. For JICF, energy distributions in

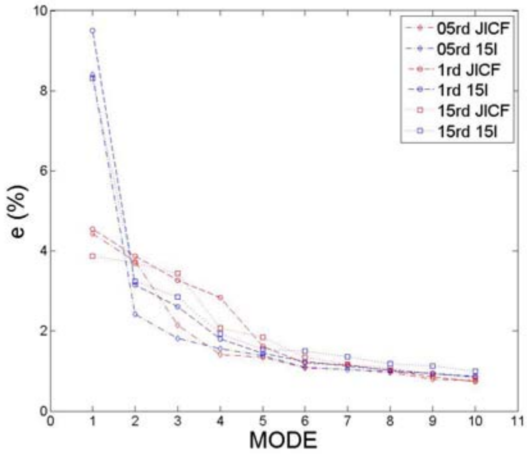

Fig. 4. Distribution of mode energy for the first ten modes and for planes *x/rd* = 0.5, 1 and 1.5.

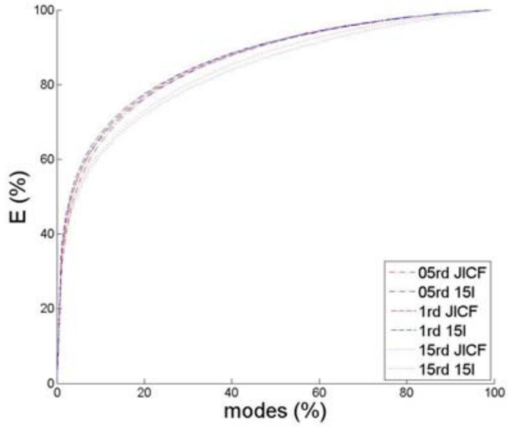

Fig. 5. Percentage of accumulative energy in lower modes to total energy for planes *x/rd* = 0.5, 1, and 1.5.

all planes are low-profile and broad. To give a specific example, for example, the energy of mode 1 is comparable to that of mode 2. This indicates that the energy is broadly distributed among modes in JICF.

When the control jets are applied (I15), however, energy distributions in all planes become relatively high-profile and narrow. To give a specific example, the energy of the most dominant mode, mode 1, is approximately three times of mode 2. This indicates that the energy becomes relatively concentrated in the first few modes when compared to JICF. In other words, this shows that the control jets have an effect in promoting and energizing a few dominant modes, in this case mode 1, over other modes when compared to JICF.

Finally, since this is the distribution of the percentage of mode energy to total energy of the velocity fluctuation among modes, it should be interpreted as such. For example, the results do not imply any relative magnitude of the absolute energy between JICF and I15 (e.g., the results do not indicate that the energy of mode 1 of I15 is twice as large as mode 1 of JICF).

Figure 5 shows the percentage of accumulative energy in the lower modes to total energy (E , i.e., the percentage of the sum of energy of all lower m modes to the total energy of all modes) in relation to the percentage of the number of lower modes (i.e., the percentage of the lower m modes to the total number of modes). For all cases and all planes, the percentage of accumulative energy in lower modes to total energy increases drastically to about 50% in the first 5% of lower modes. In other words, half of the total energy contains in the lower 5% of modes.

4. Conclusion

The effects of azimuthal control jets on the structures of a jet in crossflow are investigated by POD analysis performed on the 'jet' fluctuating velocity in which the time mean is subtracted.

Note that the jet here is referred to the region in which its volume is at least partly composed of the main jet fluid.

It is found that when the control jets are applied (I15), the most dominant structures change significantly. This is accompanied by the redistribution of energy among modes: from broad and low-profile in JICF to narrow and high-profile in I15. In other words, when the control jets are applied, the energy becomes more concentrated in the first few modes when compared to JICF. This indicates that the control jets have an effect in promoting and energizing a few dominant modes or structures, in this case mode 1, over other modes when compared to JICF.

5. Acknowledgement

The assistance of Mr. Taned Witayaprapakorn in help setting up the system and acquiring data are acknowledged and appreciated. The project is partly funded by the Five-Year Bachelor-Master degree program of the Department of Mechanical Engineering, Faculty of Engineering, Chulalongkorn University, in which the first author is enrolled; the funding is acknowledged.

References

[1] Smith, S. H. and Mungal, M. G. (1998). Mixing, structure and scaling of the jet in crossflow, *J. Fluid Mech.*, Vol. 357, pp. 83-122.

[2] Yuan, L. L., Street, R. L., and Ferziger, J. H. (1999). Large-eddy simulation of a round jet in crossflow, *J. Fluid Mech.*, Vol. 379, pp. 71-104.

[3] Bunyajitradulya, A. and Sathapornnanon, S. (2005). Sensitivity to tab disturbance of the mean flow structure of nonswirling jet and swirling jet in crossflow, *Phys. Fluids 17*, 045102.

[4] Yuan, L. L. and Street, R. L. (1998). Trajectory and entrainment of a round jet in crossflow, *Phys. Fluids*, Vol. 10, No. 9, pp. 2323-2335.

[5] Chongsiripinyo K., Limdumrongtum P., Pimpin A., and Bunyajitradulya A. (2008). Investgation of mixing structure in the near field of a jet in crossflow. Proceedings of The Twenty-Second Conference of Mechanical Engineering Network of Thailand, 15-17 October 2008, Thammasat University, Rangsit Campus, Pathum Thani, Thailand.

[6] Limdumrongtum P., Chongsiripinyo, K., Nontiwatwanich, Pimpin A., and Bunyajitradulya A. (2009). Investigation of mixing structure in the near field of swirling jets in crossflow. Proceedings of The Twenty-Third Conference of The Mechanical Engineering Network of Thailand, November 4-7, 2009, Chiang Mai.

[7] Watakulsin, P., Gimjaiyen, W., Saengnumpong, W., Sangnimnuan, A., Pimpin, A., and Bunyajitradulya, A. (2010). Effect of effective velocity ratio on the near-field mixing structures of a jet in crossflow. The First TSME International Conference on Mechanical Engineering, October 20-22, 2010, Ubon Ratchathani, Thailand.

[8] Yingjaroen, T., Pimpin, A., and Bunyajitradulya, A. (2006). Evolution of Mixings Regions in Jet and Swirling Jet in Crossflow: An Experimental Study.

Proceedings of The Twentieth Conference of The Mechanical Engineering Network of Thailand, Nakhon Ratchasima, Thailand, 18-20 October 2006, TSF032.

[9] Zaman, K. B. M. Q. and Foss, J. K. (1997). The effect of vortex generators on a jet in a crossflow. *Phys. Fluids*, Vol. 9, pp. 106-114.

[10] Niederhaus, C. E., Champagne, F. H., and Jacobs, J. W. (1997). Scalar transport in a swirling transverse jet. *AIAA J.*, Vol. 35, No. 11, pp. 1697-1704.

[11] Wangjiraniran, W. and Bunyajitradulya, A. (2001). Temperature distribution in non-zero circulation swirling jet in crossflow. Proceedings of The Fifteenth Conference of The Mechanical Engineering Network of Thailand, November 28-30, 2001, Bangkok, Thailand, Vol. 1, pp. TF104-TF116.

[12] Denev, J. A., Fröhlich, J., and Bockhorn, H. (2009). Large eddy simulation of a swirling transverse jet into a crossflow with investigation of scalar transport. *Phys. Fluids 21*, 015101.

[13] Hermanson, J. C., Wahba, A., and Johari, H. (1998). Duty-cycle effects on penetration of fully modulated, turbulent jets in crossflow. *AIAA J.*, Vol. 36, No. 10, pp. 1935-1937.

[14] Eroglu, A. and Breidenthal, R. E. (2001). Structure, penetration, and mixing of pulsed jets in crossflow. *AIAA J.*, Vol. 39, No. 3, pp. 417-423.

[15] M'Closkey, R. T., King, J. M., Cortelezzi, L., and Karagozian, A. R. (2002). The actively controlled jet in crossflow. *J. Fluid Mech.*, Vol. 452, pp. 325-335.

[16] Kornsri, P., Pimpin, A., and Bunyajitradulya A. (2009). A scheme for the manipulation and control of a jet in crossflow: The use of azimuthal control jets. The Twenty-Third Conference of the Mechanical Engineering Network of Thailand, November 4 – 7, 2009, Chiang Mai.

[17] Meyer, K.E., Pedersen, J. M., and Özcan, O. (2007). A turbulent jet in crossflow analysed with proper orthogonal decomposition. *J. Fluid. Mech.*, vol. 583, pp.199-227.